AAPS PharmSciTech (2024) 25:191
https://doi.org/10.1208/s12249-024-02913-8

RESEARCH ARTICLE

Design and Evaluation of Ophthalmic Thermosensitive *In Situ* Gel of Compound *Salvia*

Yanqiu Long[1] · Fang Lei[1] · Jie Hu[1] · Zhiyun Zheng[1,2,3,4] · Shuangying Gui[1,2,3,4] · Ning He[1,2,3,4]

Received: 4 April 2024 / Accepted: 1 August 2024

Abstract

The compound *Salvia* Recipe has been shown to have a relatively significant curative effect in management of cardiovascular and cerebrovascular diseases. This work aimed to prepare a thermosensitive *in situ* gel (ISG) delivery system that utilizes Poloxamer 407, Poloxamer 188, and hydroxypropyl methylcellulose for ocular administration of the compound *Salvia* recipe to treat cardiovascular and cerebrovascular diseases. The central composite design-response surface method was utilized to improve the prescription of the gel. The formulated gel was characterized and assessed in terms of stability, retention time, *in vitro* release, rheology, ocular irritation, pharmacokinetics studies, and tissue distribution. The gel was a liquid solution at room temperature and became semisolid at physiological temperature, prolonging its stay time in the eye. Pharmacokinetics and tissue distribution experiments indicated that thermosensitive ISG had enhanced targeting of heart and brain tissues. Additionally, it could lower drug toxicity and side effects in the lungs and kidneys. The compound *Salvia* ophthalmic thermosensitive ISG is a promising drug delivery system for the management of cardiovascular and cerebrovascular illnesses.

Keywords Compound *Salvia* recipe · Ocular administration · Pharmacokinetics · Thermosensitive *in situ* gel · Tissue distribution

Introduction

The compound *Salvia* recipe comprises *Salvia miltiorrhiza*, *Panax notoginseng*, and borneol [1, 2]. As the monarch drug (Jun in Chinese), *Salvia miltiorrhiza* has the advantages of promoting blood flow, dredging collaterals, regulating the circulation of Qi, and alleviating pain [3, 4]. *Panax notoginseng*, the minister drug (Chen in Chinese), has effects that are similar to those of *Salvia miltiorrhiza*; hence, their combination leads to synergistic interactions that can double their effectiveness[5, 6]. Borneol acts as both an assistant (Zuo in Chinese) and a guide (Shi in Chinese), and its effects include awakening enlightenment, clearing heat, and reducing swelling. Borneol can promote the passage of drugs through the blood–brain barrier [7, 8]. Related pharmacological research has shown that the compound *Salvia* recipe has anti-myocardial ischemia properties, reduces thrombosis, reduces the effects of atherosclerosis, among others, and has been utilized to treat coronary heart disease, angina pectoris [9, 10].

The pharmacodynamic substance base of the compound *Salvia* recipe is lipophilic diterpenoids, hydrophilic phenolic acids, and *Panax notoginseng* saponins [11, 12]. The potential of water-soluble components of *Salvia miltiorrhiza* in cardiovascular diseases treatment have been explored. The efficacy of *Salvia miltiorrhiza* water-soluble ingredients is much higher than that of its lipid-soluble components. It also contributes to the dissolution and content stability of *Salvia miltiorrhiza* ingredients when *Panax notoginseng* and *Salvia miltiorrhiza* are co-decocted [13]. We previously studied the water extraction processes of *Salvia miltiorrhiza* and *Panax notoginseng* [14]. In this study, danshensu (Dss) and ginsenoside Rg_1 (Rg_1) were

✉ Ning He
hening0826@126.com

1 Department of Pharmaceutics, College of Pharmacy, Anhui University of Chinese Medicine, 350 Longzihu Road, Hefei, AnHui, People's Republic of China

2 Institute of Pharmaceutics, Anhui Academy of Chinese Medical Sciences, Hefei 230012, People's Republic of China

3 Anhui Province Key Laboratory of Pharmaceutical Preparation Technology and Application, Hefei 230012, China

4 Institute of Pharmaceutics, Anhui Academy of Chinese Medical Sciences, Hefei 230012, China

Published online: 20 August 2024

selected as the assessment indexes based on the guidelines for content determination of the compound *Salvia miltiorrhiza* dropping pills in the Chinese Pharmacopoeia and our preliminary pharmacokinetic findings in rats.

There are two pathways of ocular absorption of drugs: the corneal and non-corneal pathways. The drug transcorneal pathway is mainly used for local absorption in the eye. The non-corneal route mainly involves trans-conjunctival and trans-scleral absorption. The trans-ocular passage of the drug into the bloodstream involves through the conjunctiva, nasolacrimal duct drainage, passing through the blood-water barrier after entering the aqueous humor, and passing through the blood-retinal barrier after entering the posterior segment of the eye, among other [15–17]. Chiou aimed to deliver drugs through the eye (such as insulin), confirming that drugs can be absorbed into the bloodstream through this route[18]. Huang *et al.* [19] had mentioned that it was feasible to achieve systemic effects by trans-ocular administration in ophthalmic physiology. It has been found that around 80% of topically administered eye drops are absorbed into systemic circulation [20, 21]. Additionally, it has been reported in the literature that some eye preparations can induce heart-related diseases [22, 23]. This research group has previously studied the systemic transport of drugs, such as tetramethylpyrazine hydrochloride, nimodipine, and flunarizine hydrochloride after ocular administration [24–28]. Their results confirmed the feasibility of treating systemic diseases after ocular administration; compared with oral administration, some drugs were found to have high bioavailability and good brain targeting after ocular administration.

The eye dosage form of ophthalmic drops are more commonly used**;** however, the bioavailability of eye drops is generally low [29]. ISG is a class of drug delivery systems consisting of polymer delivery carriers that deliver drugs to the site of administration in a solution and undergo a sol–gel transition in physiological environments. ISG has good histocompatibility and a long retention time at the administration site, which could improve the drug's bioavailability. Thermosensitive ISG is the most common class of environmentally sensitive polymer systems [30, 31]. Wang *et al.* [32] prepared ocular diclofenac sodium hydrochloride nanoparticles in thermosensitive *in situ* gels by utilizing Poloxamer 407 (P407), Poloxamer 188 (P188), and hydroxypropyl methylcellulose (HPMC) as the gel matrix. This improved the corneal penetration ability of the drug and prolonged its retention time. ISG is expected to provide new potentials for ocular drug delivery.

In this study, a compound *Salvia* ophthalmic thermosensitive ISG (CSOT-ISG) was prepared with P407, P188, and HPMC as the gel matrix, and its characteristics were evaluated. The *in vivo* pharmacokinetics of CSOT-ISG after ocular administration were also studied to explore the feasibility of systemic transport and brain delivery of CSOT-ISG.

Materials and Methods

Materials

Salvia miltiorrhiza and *Panax notoginseng* were supplied from Anhui Huaxiu Pharmaceutical (Bozhou, China). Borneol, formic acid, and puerarin were supplied from Aladdin Biochemical Technology (Shanghai, China). Control products of Danshensu sodium and ginsenoside Rg_1 were purchased from Chengdu Durst Biotechnology (Chengdu, China). Poloxamer 407 and Poloxamer 188 were supplied from BASF (Ludwigshafen, Germany). Hydroxypropyl methyl cellulose (HPMC) was supplied from Shanghai Kalkang Packaging Technology (Shanghai, China). Benzalkonium chloride and sodium fluorescein were obtained from Jiangxi Alpha Hi-tech Pharmaceutical (Pingxiang, China). The purified water utilized in the experiments was received from a Milli-Q system. All the chemicals and reagents utilized were chromatographic or analytical grade.

Animals

Animal experiments were reviewed and approved by the Animal Management and Ethics Committee of Anhui University of Chinese Medicine (Anhui, China; approval numbers AHUCM-rats-2021097 and AHUCM-rabbits-2021132). The experimental **processes were** strictly implemented in accordance with the regulations of the Animal Experimental Center of Anhui University of Chinese Medicine.

Healthy male New Zealand white rabbits (2.5–3.0 kg) were got from Huaxing Experimental Animal Farm (Zhengzhou, China), while healthy adult male SD rats (200 ± 20 g) were got from Pizhou Oriental Breeding. The animals were placed in animal cages with water and standard chow. All animals were free of ocular abnormalities.

Analytical Methods

Ultra-High-Performance Liquid Chromatography (UHPLC)

The instrument consisted of an Accucore™ C18 (2.6 μm, 4.6 mm × 100 mm) analytical column. Mobile phase: acetonitrile (A)—0.2% (v/v) phosphate water (B); flow rate: 0.3 mL/min; detection wavelength: 280 nm (Danshensu); 203 nm (Rg_1); column temperature: 30 °C; sample intake: 1 μL. The gradient conditions were as follows: 5% A at 0–6 min, 5–21% A at 6–8 min, 21–25% A at 8–11 min, 25–33% A at 11–18 min, and 33–40% A at 18–28 min. For Danshensu: the concentration range was 25–600 μg/mL, and

Table I Calibration Curves of Dss and Rg_1 in Plasma and Various Tissues of Rats

Compound	Sample	Calibration curve	R^2	concentration range ng/mL(g)	LLOQ ng/mL(g)
Rg_1	plasma	$Y=0.0317\,X+0.1692$	0.997	0.5 ~ 250	0.5
	brain	$Y=0.0361\,X+0.1436$	0.999	0.5 ~ 100	0.5
	heart	$Y=0.0277\,X+0.1712$	0.997	0.5 ~ 250	0.5
	liver	$Y=0.0228\,X+0.1769$	0.998	0.5 ~ 250	0.5
	spleen	$Y=0.0202\,X+0.1868$	0.996	0.5 ~ 100	0.5
	lung	$Y=0.0323\,X+0.1567$	0.999	0.5 ~ 500	0.5
	kidney	$Y=0.0285\,X+0.1017$	0.992	0.5 ~ 250	0.5
Dss	plasma	$Y=0.0357\,X-0.4469$	0.995	5 ~ 500	5
	brain	$Y=0.0457\,X-0.0765$	0.999	5 ~ 250	5
	heart	$Y=0.0392\,X-0.1323$	0.993	5 ~ 250	5
	liver	$Y=0.0292\,X+0.0794$	0.998	5 ~ 500	5
	spleen	$Y=0.0468\,X+0.0937$	0.997	5 ~ 250	5
	lung	$Y=0.0375\,X+0.0947$	0.999	5 ~ 250	5
	kidney	$Y=0.0400\,X-0.3171$	0.991	5 ~ 500	5

the method had good linearity ($R^2=0.9999$); the relative standard deviation (*RSD*) of precision analyses was 1.10%, while the average accuracy was 101.41%. For Rg_1: the concentration range was 25–600 μg/mL, and the method had good linearity ($R^2=0.9999$); the *RSD* of precision analyses was 0.29%; and the average accuracy was 98.67%.

Ultra-High-Performance Liquid Chromatography Coupled with Tandem Mass Spectrometry (UHPLC-MS/MS)

An UltiMate 3000 HPLC system (Thermo Fisher, Waltham, MA, USA) was used. Chromatographic conditions: column Agilent C18 column (100 mm × 2.1 mm, 1.8 μm); mobile phase: acetonitrile (A)—0.05% (v/v) formic acid water (B); flow rate: 0.3 mL/min; autosampler temperature: 4 °C; column temperature: 35 °C. These were the gradient conditions: 20–38% A at 0–1.70 min, 38–55% A at 1.70–2.00 min, 55–60% A at 2.00–3.00 min, 60–20% A at 3.00–3.01 min, and 20% A at 3.01–6.00 min.

Mass spectrometry conditions were electrospray ion source (ESI). ESI was operated simultaneously in the positive (ESI^+) and negative (ESI^-) electrospray ionization modes with the detection of multiple reaction monitoring (MRM). Dss and puerarin [27] (GGS, internal standard) adopted a negative electrospray ionization mode, whereas Rg_1 was in a positive electrospray ionization mode. The ESI configuration was that positive and negative voltages of the capillary were 4.5 kV and 5.5 kV, respectively. The curtain gas, GS1, and GS2 were set at 25 psi, 55 psi and 55 psi, respectively. Source temperature: 500 °C; scan time: 200 ms. The detection pairs of GGS, Dss, and Rg_1 were 415.2 → 267.0, 197.1 → 134.9, and 823.7 → 643.6, with collision energy voltages of -47 eV, -23 eV, and 53 eV, and declustering potentials of -101 V, -67 V, and 170 V, respectively.

Table I shows the calibration curves for each tissue sample obtained according to the sample treatment method applied.

Preparation of CSOT-ISG

Preparation of Compound *Salvia* Recipe Water-Extract Solution [14]

The herbal medicine (90 g of *Salvia miltiorrhiza* and 17.6 g of *Panax notoginseng*) were placed in a casserole with 10 times amount of water, soaked for 45 min, and then decocted three times for 2.5 h each. The decoction was filtered through gauze. The filtrate was centrifuged, and the supernatant was concentrated to 100 mL. The pH of the concentrate was adjusted to 8.0 ~ 8.5 after secondary alcohol precipitation (primary alcohol content up to 75%, secondary alcohol content up to 85%), and then the pH was adjusted to 2.5 ~ 3.0 after water precipitation**.** Finally, the liquid was filtered to obtain the water-extract solution. The pH of the water-extract solution was adjusted to neutral, and the solution was concentrated to 100 mL, followed by the addition of 1 g of borneol, and stored at 4 °C.

Preparation of Thermosensitive *In Situ* Gel

The thermosensitive *in situ* gel was made by applying the cold melting method [33]. A fixed amount of pure water was added to the beaker, and then the prescribed quantities of P407, P188, and HPMC were carefully poured into it. The polymer solution was then left at 4 °C until clarification and

Table II Factors and Levels of Central Composite Design

Factor	Level				
	−1.732	−1	0	+1	+1.732
X_1 (P407), %	17	17.85	19	20.15	21
X_2 (P188), %	0	1.69	4	6.31	8
X_3 (HPMC), %	0	0.21	0.5	0.79	1

transparency were achieved. Benzalkonium chloride (0.01%, w/w) and 50% (w/w) of compound *Salvia miltiorrhiza* extract solution were added to the polymer solution. The thermosensitive *in situ* gel was then stored in a refrigerator.

Optimization of the Formulation

The CSOT-ISG composition was improved by applying the central composite design-response surface methodology (CCD-RSM). A CCD was conducted on the three independent variables (X_1: P407 concentration ranging from 17 to 21% (w/w); X_2: P188 concentration ranging from 0 to 8% (w/w); X_3: HPMC concentration ranging from 0 to 1% (w/w)) at five coded levels: -1.732, -1, 0, + 1, and + 1.732 (Table II). Dependent variables T_1 and T_2 were the gelation temperature (GT) of the CSOT-ISG before and after artificial tears (STF) dilution. The artificial tears was prepared by dispersing 0.678 g of sodium chloride, 0.008 g of calcium chloride dihydrate, 0.218 g of sodium bicarbonate**,** and 0.138 g of potassium chloride into 100 mL of distilled water [34]. CCD experiments were conducted utilizing Design-Expert 8.0.6 software. The quadratic polynomial fitting to the results and the contour and three-dimensional response surface maps of various factors on T_1 and T_2 were drawn.

Characterization of CSOT-ISG

To characterize CSOT-ISG, the following methods were used. The appearance of CSOT-ISG was investigated, and the pH values were tested using a pH meter (PHSJ-4A, Hinotek, Shanghai, China). The test tube inversion method was adopted to measure the GT. The viscosity of the gel was determined by a digital display viscometer (Brookfield DV2TRV, Stoughton, MA, USA) with a No. 3 spindle at a speed of 30 rpm at 25 °C (before artificial tears dilution) and 35 °C (after artificial tears dilution). Dss and Rg_1 contents in the gel were determined by UHPLC.

Rheological Studies [35–37]

When droped into the eye, thermosensitive gel undergo a phase transition due to changes in temperature, transitioning from a flowing liquid to a viscoelastic gel. Therefore, the rheological study of CSOT-ISG is essential. The rheology of CSOT-ISG was studied utilizing a Discover DHR-2 rheometer (TA instruments, New Castle, DE, USA). A 20 mm diameter cone-plate (cone angle: 1°) was utilized in this study. The thermosensitive gel sample mass was approximately 200 mg each time.

Viscosity Test

The CSOT-ISG before and after artificial tears dilution underwent to a steady-state shear scan in the Flow-sweep mode to determine the relationship between shear rate and viscosity. Test conditions were set to 0.01–100 s^{-1} for shear rates.

In the Flow Temperature Ramp mode, this study examined how gel viscosity changes as temperature increases. Test conditions were set to 100 s^{-1} for shear rate, 10–45 °C for temperature range, and 5 °C/min for heating rate.

Frequency Sweep Test

Small amplitude frequency scanning was performed on CSOT-ISG before and after artificial tears dilution applying the Oscillation Frequency mode to examine the changes in CSOT-ISG's viscoelasticity as angular frequency increased. Test conditions were set to 0.01–100 rad/s for frequency, and 0.1% for strain.

Investigation of the Erosion and Release Behavior of CSOT-ISG

The *in vitro* release and erosion of CSOT-ISG were researched by the membrane-less dissolution method [38]. A weighed Eppendorf (EP) tube containing 1 mL of CSOT-ISG solution was placed in a constant-temperature water bath at 35 °C with a rotation speed of 100 r/min until the gel was completely formed. The total weight of CSOT-ISG and EP tubes was recorded. Fresh artificial tears were then added to the EP tube with a volume of 2 mL. Afterwards, 2 mL of artificial tears in the EP tube were poured out at specific time points (20, 60, 100, 140, 200, 320, 440, and 560 min). The surface of the EP tube was wiped, and the mass was weighed and recorded. Furthermore, 2 mL of fresh artificial tears were added to the EP tube again and poured out at the next specified time point until the gel's weight in the EP tube was less than 10% of the original weight. The differences in gel weight between each pair of adjacent time points were calculated to evaluate the erosion amount of the gel, and the cumulative erosion rate was calculated. The cumulative erosion rate was the ratio of the cumulative erosion mass to the initial mass of CSOT-ISG. This experiment was repeated thrice.

At each time point, artificial tears poured out were diluted using pure water before being passed through microporous membranes, according to the UHPLC method, to determine the contents of Dss and Rg_1 and to calculate the cumulative release rate.

Stability Studies

CSOT-ISG were underwent stability studies in a variety of conditions, including centrifugation (3500 r/min, 20 min), light (4,500 ± 500 Lx), and storage temperatures (4 °C or 25 °C). The light stability experiment was performed in a light box with a light intensity of 4500 Lx ± 500 Lx and the CSOT-ISG was withdrawn on the 0th, 5th and 10th days. To evaluate the stability at different temperatures, CSOT-ISG was withdrawn from the well-sealed vials at 0, 5 and 10 days after storage at 4 °C and 25 °C. Key indicators including GT, appearance, and Dss and Rg_1 loading contents were determined to assess stability. The stability testing was performed three times in parallel.

Ocular Fluorescence Retention Test

Sodium fluorescein (0.1%) was contained into CSOT-ISG (experimental group) and normal saline (control group). A dosages of 50 µL of CSOT-ISG and normal saline were separately absorbed into the rabbits' right and left conjunctival sacs. The fluorescein intensity was observed and recorded by gently pulling down the eyelids of the subjects every 5 min.

Histology

The effects of repeated administrations on ocular tissue structures were examined. The compound *Salvia* solution ophthalmic drops, or CSOT-ISG, were absorbed into the left eyes of rabbits multiple times, and a control was created by dripping normal saline into the right eyes. The rabbits were immediately euthanized, and their eyeballs were extracted. Afterwards, separation of the cornea, iris, and conjunctiva was carried out. These tissues were fixed in 4% paraformaldehyde, paraffin embedded, sectioned, and stained using hematoxylin and eosin. An optical microscope (Olympus, BX43, Japan) was then applied to visually assess pathological alterations.

Pharmacokinetics

A total of 135 Sprague–Dawley rats were split into a compound *Salvia* solution intragastric group, a compound *Salvia* solution ophthalmic drop group, and a CSOT-ISG group with 45 rats in each group. The three groups were administered the same doses (equivalent to 3.165 mg/kg of Dss, 1.823 mg/kg of Rg_1, and 3.184 mg/kg of borneol). At predetermined time points (2, 5, 15, 30, 60, 90, 120, 180, and 540 min) after dosing (five animals per time point, n = 5), rats were sacrificed through femoral artery bleeding, and blood samples were collected while the tissues (heart, brain, liver, spleen, lungs, and kidneys) were collected. Blood samples were placed into heparinized centrifuge tubes and spun at 3500 rpm for 10 min. Afterwards, 100 µL of plasma were added in 10 µL of the IS solution (200 ng/mL), and samples were vortexed for 1 min before 50 µL of formic acid (1%) was added and mixed. Following the addition of 2 mL of *N*-butyl alcohol-ethyl acetate (1:4, v/v), samples were vortex-mixed at 3000 rpm for 9 min. After centrifugation for 10 min at 4500 rpm, the supernatant was pipetted onto an EP tube. The EP tube was dried under nitrogen at 25 °C. The original mobile phase ratio of 100 µL was used to reconstitute the residue. The solution then underwent 3 min of vortexing, 2 min of sonication, and 10 min of centrifugation at 15000 rpm. The supernatant was placed in an injection bottle. Tissue samples were washed with physiologic saline to remove blood from their surfaces, while superficial connective tissues were removed using forceps [24]. Afterwards, absorbent paper was used to gently dry the tissues. Homogenate was created by weighing the tissues and breaking them with physiologic saline (1:2, m/v). Afterwards, 100 µg of homogenate was accurately weighed, and the subsequent treatment steps were the same as those for plasma samples. UHPLC-MS/MS was applied to measure the amounts of Dss and Rg_1 in plasma and each tissue sample. The average concentrations of Dss and Rg_1 in plasma or each tissue were calculated.

The pharmacokinetic parameters of Dss and Rg_1 in rat plasma and tissues were calculated by DAS 2.0 software. A one-way analysis of variance on the pharmacokinetic parameters of each group was performed using SPSS 23.0 software to identify statistical differences, with $P < 0.05$ denoting statistically significant difference. All results were presented as mean ± *SD*. For each tissue, the targeting index (*TI*), targeting efficiency (*Te*) and relative targeting efficiency (*Rte*) of the ophthalmic drop group in comparison to those of the intragastric group were calculated according to Eq. (1), Eq. (2),and Eq. (3) [39, 40]. The *TI*, *Te*, and *Rte* of the CSOT-ISG group in comparison to the ophthalmic drop group were also calculated.

$$TI = AUC_{\mathrm{i}\ traget}/AUC_{\mathrm{i}\ reference} \tag{1}$$

$$Te = AUC_{\mathrm{i}\ traget}/\sum_i^n AUC_{\mathrm{i}\ reference} \tag{2}$$

$$Rte = \left(Te_{traget} - Te_{reference}\right)/Te_{reference} \tag{3}$$

where i is the i^{th} tissue and the $\sum_i^n AUC_{\mathrm{i\ reference}}$ is the sum of the *AUC* for all tissues, including the target tissues. The

$AUC_{0\text{-}t}$ is the mean area under the curve from time 0 to t. The larger the *Te*, the more the drug is distributed in the tissue. If the *TI* is greater than 1 or *Rte* is greater than 0, the CSOT-ISG group displays more tissue targeting than the ophthalmic drop group or the ophthalmic drop group displays more tissue targeting than the intragastric group.

Results

Optimization of CSOT-ISG

To optimize the CSOT-ISG's formulation, twenty experiments were planned according to the CCD-RSM to test three factors at five levels (Table III). The following models were obtained:

$$T_1 = 18.65 - 3.03X_1 + 2.20X_2 - 0.61X_3 - 0.17X_1X_2 + 0.088X_1X_3 - 0.19X_2X_3 + 0.49X_1^2 - 0.15X_2^2 + 0.094X_3^2 \ (R^2 = 0.9952, P < 0.0001)$$

$$T_2 = 28.55 - 3.33X_1 + 3.26X_2 - 0.37X_3 + 0.34X_1X_2 + 0.24X_1X_3 + 0.11X_2X_3 + 0.16X_1^2 - 1.14X_2^2 - 0.025X_3^2 \ (R^2 = 0.9946, P < 0.0001)$$

Based on the R^2-values and P-values of the above two model equations, the model equations were significant and displayed a good fit, and can be used for the analysis and prediction of T_1 and T_2. Figure 1 illustrates that T_1 and T_2 decreased with rising P407 and HPMC concentrations, while T_1 and T_2 increased with expanding in P188 concentration. The intensity of the contour map was X_1X_2 (P407, P188) > X_1X_3 (P407, HPMC) > X_2X_3 (P188, HPMC), which meant the strength of the factor interaction was $X_1X_2 > X_1X_3 > X_2X_3$. After screening and validation, the optimal concentrations of P407, P188 and HPMC were set to 17.85%, 6.31%, and 0.21%, respectively. The T_1 and T_2 in the optimized CSOT-ISG were verified to be 25.83 ± 0.15 °C and 34.17 ± 0.31 °C, respectively.

Characterization of CSOT-ISG

The visual evaluation of the CSOT-ISG proved that the gel was orange-yellow, clear, and transparent when exposed to light (Fig. 2). It was liquid at ambient temperature and became semi-solid at 35 °C (after dilution with artificial tears). The pH value (6.97 ± 0.05) of the CSOT-ISG met the requirements for ophthalmic preparations, as did the GT and viscosity. Dss and Rg_1 had respective contents of 4.22 ± 0.04 mg/mL and 2.43 ± 0.02 mg/mL.

Table III Design and Results of Central Composite Design

Number	P407 (X_1, %)	P188 (X_2, %)	HPMC (X_3, %)	T_1 /°C	T_2 /°C
1	17.85	1.69	0.21	20.2	28.5
2	20.15	1.69	0.21	14.3	21.1
3	17.85	6.31	0.21	25.1	34.3
4	20.15	6.31	0.21	19.1	27.3
5	17.85	1.69	0.79	19.1	27.2
6	20.15	1.69	0.79	14.1	19.8
7	17.85	6.31	0.79	23.8	32.5
8	20.15	6.31	0.79	17.6	27.4
9	17.01	4.00	0.50	25.7	35.1
10	20.99	4.00	0.50	14.5	23.7
11	19.00	0.00	0.50	14.4	19.5
12	19.00	8.00	0.50	21.9	31.5
13	19.00	4.00	0.00	20.2	29.1
14	19.00	4.00	1.00	17.6	28.6
15	19.00	4.00	0.50	19.6	28.5
16	19.00	4.00	0.50	18.2	29.1
17	19.00	4.00	0.50	18.8	28.7
18	19.00	4.00	0.50	18.5	28.1
19	19.00	4.00	0.50	18.6	28.2
20	19.00	4.00	0.50	18.5	28.7

Rheological Studies

Viscosity Test

According to Fig. 3a, the viscosity of CSOT-ISG before and after artificial tears dilution decreased significantly with an increase in shear rate, implying that the CSOT-ISG exhibited a pseudoplastic fluid state under both physiological and non-physiological conditions. When the shear rate was low, the high viscosity of the gel contributed to storage and maintained stability; when the shear rate was high, the viscosity was rapidly reduced to facilitate the gel coating the eye, thereby reducing patients' discomfort.

As the temperature increased, the viscosity of the formulations slowly increased before and after diluted using STF (Fig. 3b). If the temperature continues to rise, the sol phenomenon will occur. The results implied that GT was around 26 °C and 34 °C before and after STF dilution, respectively. Therefore, the results further demonstrated that the prepared CSOT-ISG fulfilled the ophthalmic application requirements.

Frequency Sweep Test

As shown in Fig. 3c, at lower values of angular frequencies (ω), the loss modulus (G") was greater than the storage

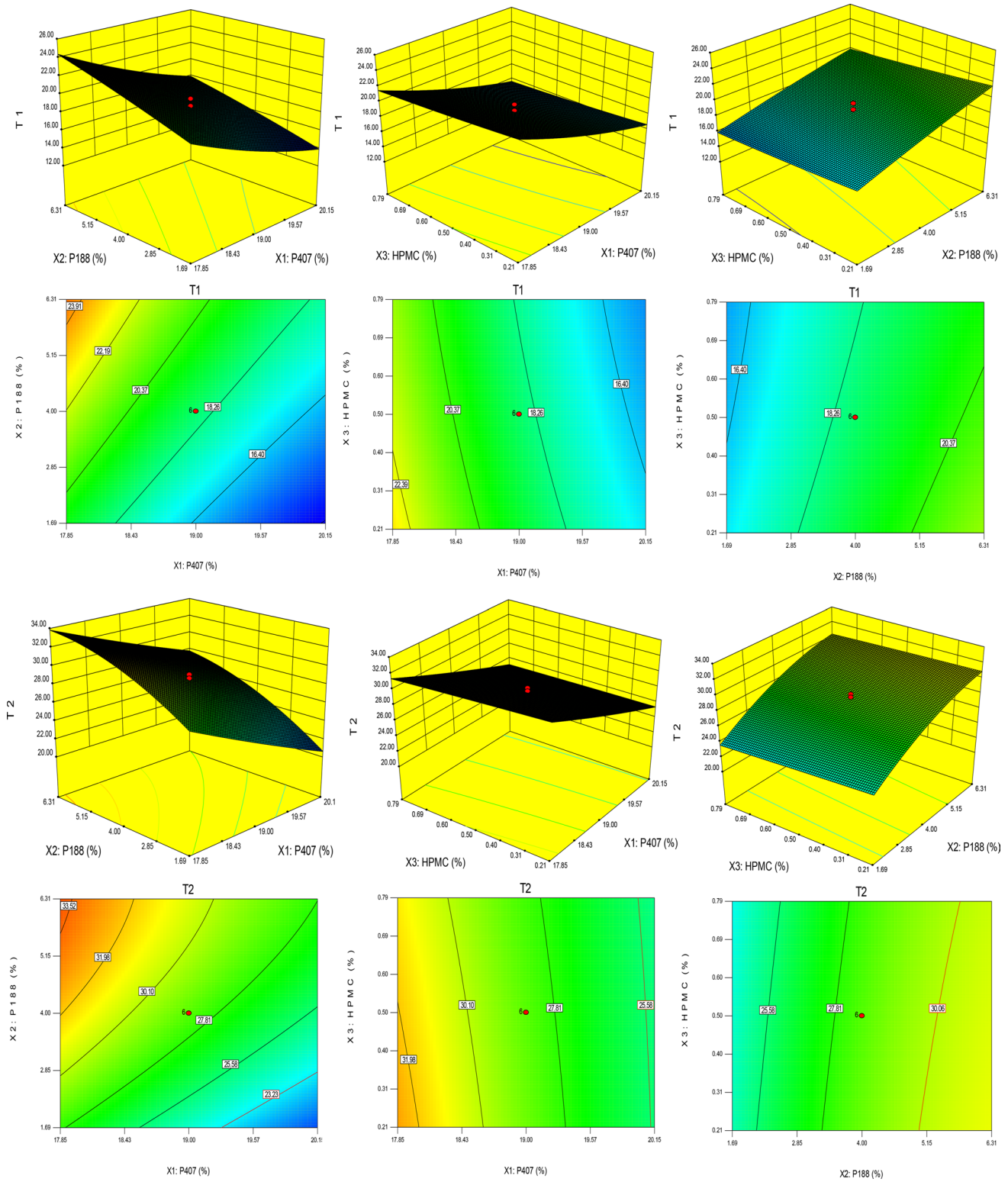

Fig. 1 Contour and three-dimensional response surface maps of various factors on T_1 and T_2

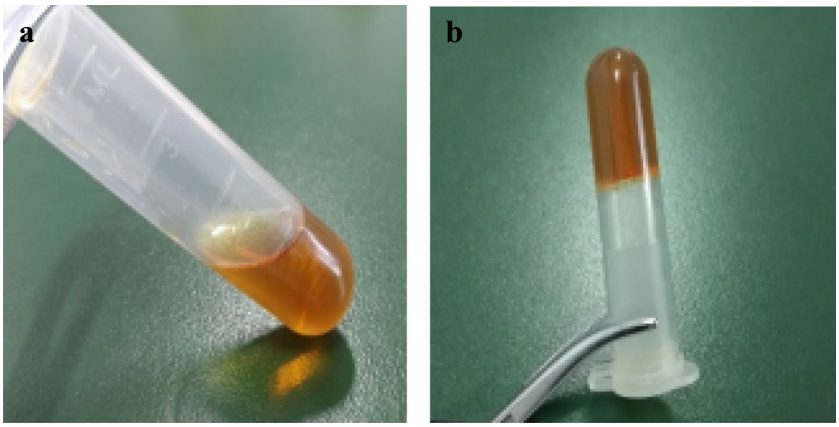

Fig. 2 Appearance of compound *Salvia* thermosensitive *in situ* gel. **a** Room temperature. **b** Artificial tears + 35 °C

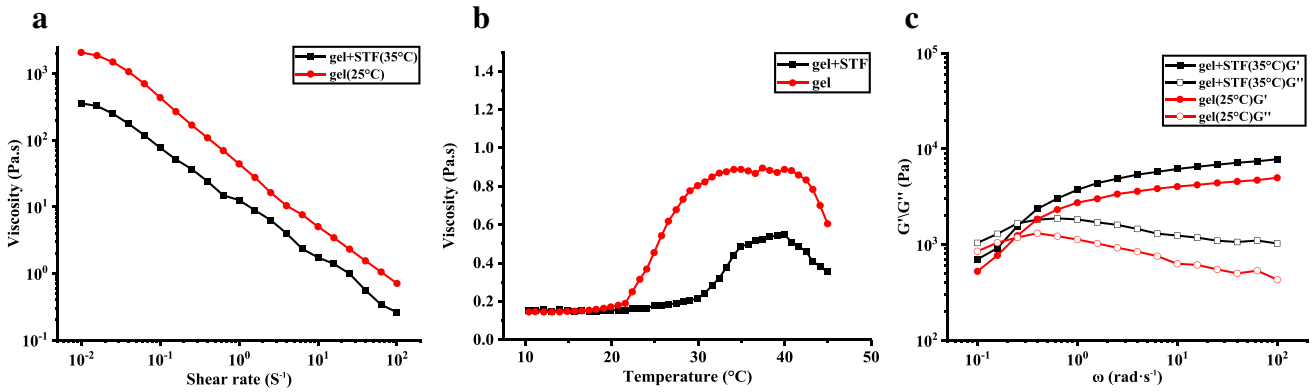

Fig. 3 Rheological study. **a** Curve of viscosity with shear rate. **b** Curve of viscosity with temperature. **c** Frequency sweeps test of gels

modulus (G') under both room temperature and physiological conditions, indicating that the gel showed a viscous flow state. At high ω values, the gel exhibited solid-state properties. In addition, the values of G' and G" under physiological conditions were greater than those at room temperature, suggesting that the gel had greater elasticity under physiological conditions, which was conducive to its retention in the eye and prolongation of drug release.

Erosion and Release Behavior of CSOT-ISG

The membrane-free dissolution method was applied in this study as it is more suitable to simulate the authentic scenario of the gel in the eye. The cumulative erosion rate exhibited good linear relations with time ($Y = 0.1625\ X + 6.879$, $R = 0.9908$; Fig. 4a), and followed a zero-order kinetic process. The cumulative release rate curve of CSOT-ISG is depicted in Fig. 4b. The cumulative release rate of Dss and Rg_1 had a linear relationship with the cumulative erosion rate (Dss: $Y = 1.0576\ X + 0.8716$, $R = 0.9985$; Rg_1: $Y = 1.0002\ X + 2.5843$, $R = 0.9993$; Fig. 4c), indicating that Dss and Rg_1 in the gel were primarily released by erosion. The best-fitting release kinetics model was the first-order model (Dss: $R^2 = 0.999$; Rg_1: $R^2 = 0.997$; Table IV).

Stability of CSOT-ISG

The stability of the CSOT-ISG was evaluated under different storage temperatures, centrifugation, and strong light irradiation conditions to ensure its stability in terms of its appearance, GT, and drug content. The gel's indexes remained unchanged after centrifugation (appearance: orange-yellow, clear and transparent; Dss content: 99.10 ± 0.10%; Rg_1 content: 99.50 ± 0.20%; GT: 34.27 ± 0.15 °C; n = 3). As shown in Table V, the gel remained stable at 4 °C, while the Dss content decreased slightly after storage at 25 °C. The GT increased slightly, and the content of Dss decreased slightly under strong light irradiation (Table V). The results implied that CSOT-ISG should be preserved at 4 °C and away from light.

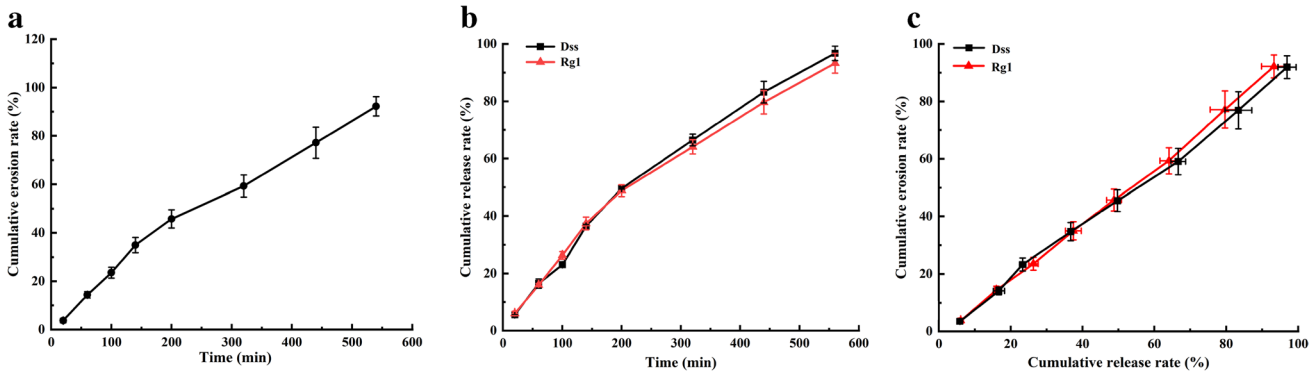

Fig. 4 **a** Cumulative erosion profile of CSOT-ISG. **b** Cumulative release profile of CSOT-ISG. **c** Cumulative erosion/release rate of drugs in CSOT-ISG

Table IV Model Simulated for the Release Profiles of COST-ISG

Compound	Type of model	Equations	R^2
Dss	Zero-order	$Q=0.2368\,t+0.8790$	0.989
	First-order	$Q=176.0586\,(1-e^{-0.0016t})$	0.999
	Higuchi	$Q=4.4739\,t^{1/2}-14.3947$	0.997
	Ritger-Peppas	$Q=0.3431\,t^{0.9331}$	0.993
Rg_1	Zero-order	$Q=0.1814\,t+4.9377$	0.959
	First-order	$Q=127.8137\,(1-e^{-0.0023t})$	0.997
	Higuchi	$Q=4.4186\,t^{1/2}-16.6209$	0.977
	Ritger-Peppas	$Q=0.6331\,t^{0.7985}$	0.987

Q is cumulative release rate, and t is time

Ocular Residence Time

As shown in Fig. 5, the fluorescence intensity of the CSOT-ISG under an ultraviolet lamp was noticeably less than that of the control group. No fluorescence was observed after approximately 10 min in the control group. In the CSOT-ISG group, no fluorescence was observed after approximately 35 min. The results demonstrated that CSOT-ISG could extend the stay time of sodium fluorescein in the eyes and decrease drug loss.

Histopathological Examination

Both the compound *Salvia* eye drop group and the CSOT-ISG group did not exhibit any appreciable histological alterations in the cornea, iris, or conjunctival tissues when compared to the normal saline group (Fig. 6), suggesting that the compound *Salvia* eye drop and CSOT-ISG could be safely administered through the ocular route.

Table V Stability Test ($n=3$)

Condition	Indicator	Time		
		0 d	5 d	10 d
4 °C	appearance	orange-yellow, clear and transparent	orange-yellow, clear and transparent	orange-yellow, clear and transparent
	GT (°C)	34.40 ± 0.10	34.43 ± 0.06	34.43 ± 0.12
	Dss content (%)	99.68 ± 0.42	99.95 ± 0.75	99.58 ± 0.06
	Rg_1 content (%)	100.12 ± 0.08	100.03 ± 0.12	100.12 ± 0.12
25 °C	appearance	orange-yellow, clear and transparent	orange-yellow, clear and transparent	orange-yellow, clear and transparent
	GT (°C)	34.43 ± 0.06	34.47 ± 0.15	34.43 ± 0.21
	Dss content (%)	99.44 ± 0.01	99.12 ± 0.49	98.29 ± 0.43
	Rg_1 content (%)	100.07 ± 0.04	100.07 ± 0.10	100.45 ± 0.50
Light	appearance	orange-yellow, clear and transparent	orange-yellow, clear and transparent	orange-yellow, clear and transparent
	GT (°C)	34.47 ± 0.15	34.60 ± 0.10	34.97 ± 0.12
	Dss content (%)	99.45 ± 0.01	99.47 ± 0.06	97.09 ± 0.61
	Rg_1 content (%)	100.13 ± 0.05	100.05 ± 0.03	100.14 ± 0.04

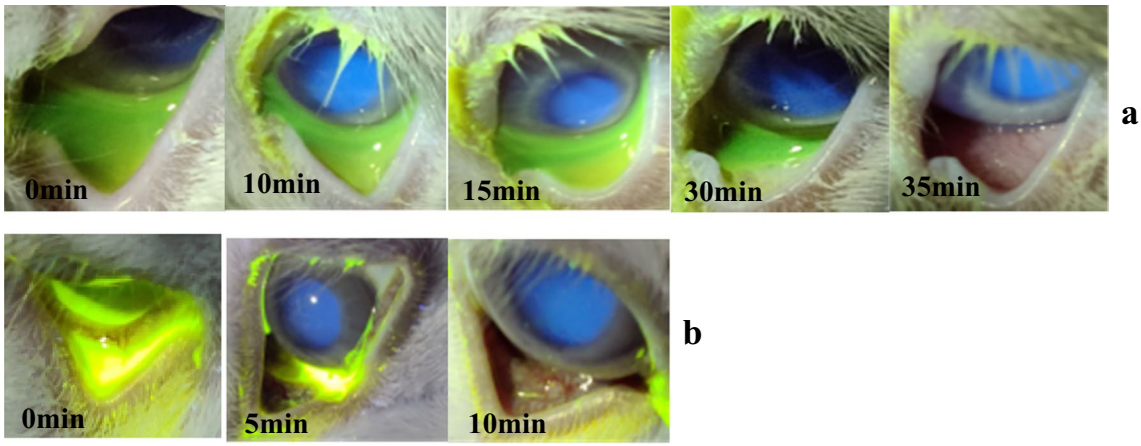

Fig. 5 Retention time of normal saline **b** and CSOT-ISG **a** in rabbit eyes

Pharmacokinetics

Pharmacokinetic Parameters in Plasma

The plasma concentration–time curves of Dss and Rg_1 are exhibited in Fig. 7. The main pharmacokinetic parameters and their significance analysis results are summarized in Table VI.

Compared to the intragastric group, the ophthalmic drop group exhibited a higher C_{max} and an earlier T_{max} of Dss in plasma. Overall, the concentration of Rg_1 in plasma in the ophthalmic drop group was higher than that in the intragastric group. Notably, the C_{max} of Rg_1 in plasma between the intragastric group (0.007 ± 0.002 mg/L) and the ophthalmic drop group (0.033 ± 0.003 mg/L) were significantly different. The $AUC_{0\text{-}t}$ of Rg_1 in plasma for the ophthalmic drop

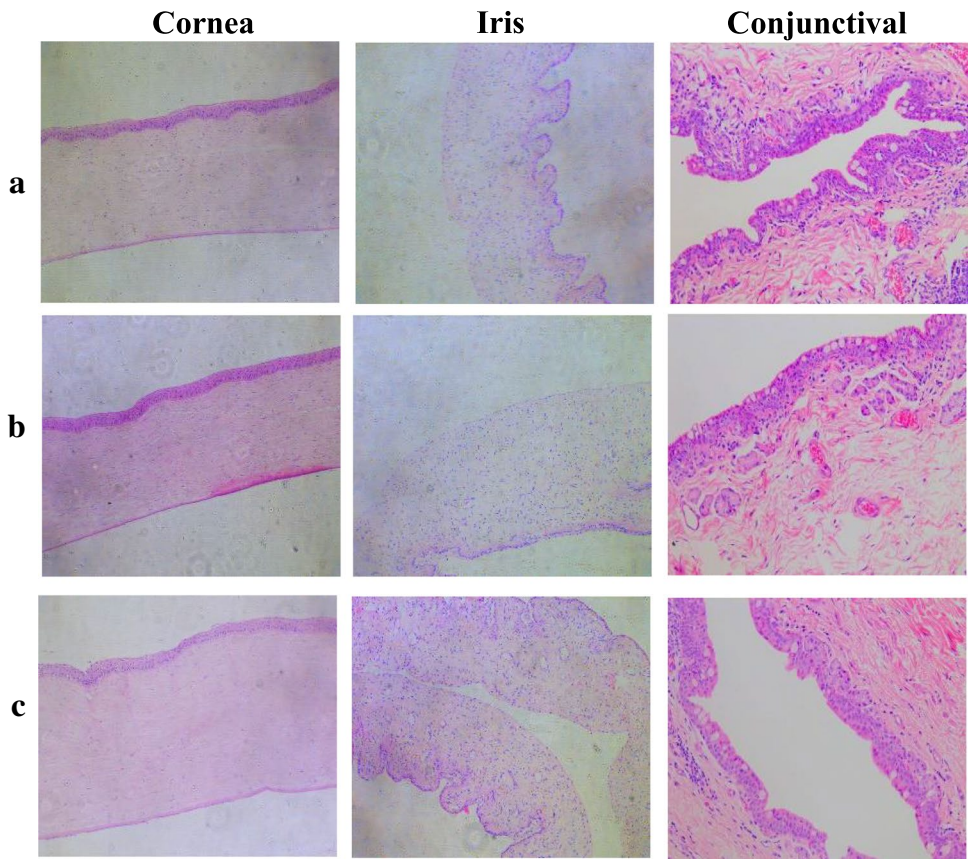

Fig. 6 Photomicrographs showing histopathological sections of rabbit eyes. (**a** normal saline group, **b** eye drop group, **c** CSOT-ISG group. Scale bar: 50 μm)

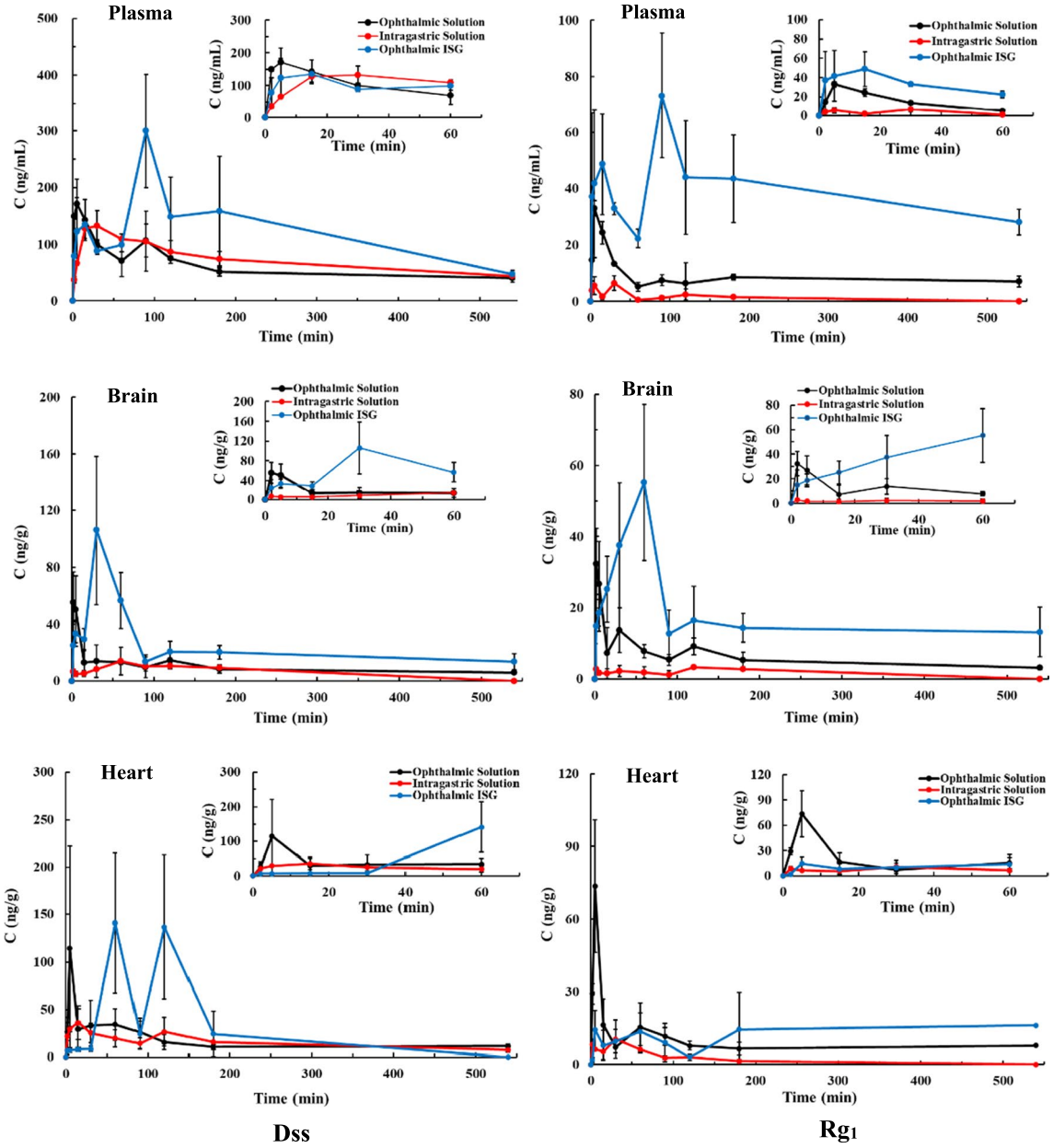

Fig. 7 Concentration–time curves of Dss and Rg_1 in biological samples (mean ± *SD*, $n = 5$)

group was 10 times higher compared to that of the intragastric group ($^{*}P < 0.05$).

Compared to the ophthalmic drop group, the CSOT-ISG group had significantly higher plasma concentrations of Dss and Rg_1. The C_{max}, $AUC_{0\text{-}t}$, and $t_{1/2}$ of Dss in the CSOT-ISG group were 0.300 ± 0.227 mg/L, 65.107 ± 12.207 mg/L·min, and 2.957 ± 1.578 h, respectively, all of which showed significant differences compared to their values in the ophthalmic drop group. The C_{max} and $AUC_{0\text{-}t}$ of Rg_1 in the CSOT-ISG group were 0.073 ± 0.018 mg/L and 20.761 ± 8.014 mg/L·min, respectively, which indicated highly significant differences when compared with their values in the ophthalmic drop group. The results illustrated that CSOT-ISG could significantly improve drug absorption after ocular delivery, extending the half-life of the drug.

Pharmacokinetic Parameters in Tissues

The average concentration *versus* time profiles of Dss and Rg_1 in the brain are plotted in Fig. 7. The relevant pharmacokinetic parameters are summarized in Table VI. The contents of Dss and Rg_1 in the brain tissue in the ophthalmic drop group were increased compared with those in the intragastric group. The $AUC_{0\text{-}t}$ (5.063 ± 0.268 mg/L·min) and

Table VI Pharmacokinetic Parameters of Dss and Rg_1 in Biological Samples (mean ± *SD*, *n* = 5)

Sample	Compound	Group	T_{max} (h)	C_{max} (mg/L)	$AUC_{0\text{-}t}$ (mg/L·min)	$t_{1/2}$ (h)
Plasma	Dss	ig	0.5	0.133 ± 0.019	38.751 ± 3.750	5.949 ± 1.881
		io-solution	0.083	0.171 ± 0.032	32.254 ± 1.160	1.461 ± 0.111*
		io-gel	1.5	0.300 ± 0.227$^{\Delta}$	65.107 ± 12.207$^{\Delta\Delta}$	2.957 ± 1.578$^{\Delta}$
	Rg_1	ig	0.5	0.007 ± 0.002	0.425 ± 0.143	0.466 ± 0.082
		io-solution	0.083	0.033 ± 0.003**	4.611 ± 0.437	2.777 ± 0.584
		io-gel	1.5	0.073 ± 0.018$^{\Delta\Delta}$	20.761 ± 8.014$^{\Delta\Delta}$	10.346 ± 3.186
Brain	Dss	ig	1	0.014 ± 0.001	1.796 ± 0.196	3.454 ± 2.041
		io-solution	0.033	0.055 ± 0.021	5.063 ± 0.268*	10.814 ± 1.853*
		io-gel	0.5	0.106 ± 0.100	12.783 ± 3.642$^{\Delta\Delta}$	11.518 ± 4.973
	Rg_1	ig	2	0.003 ± 0.001	0.414 ± 0.064	2.303 ± 0.431
		io-solution	0.033	0.032 ± 0.007	3.148 ± 0.537*	9.033 ± 1.648
		io-gel	1	0.055 ± 0.040	9.491 ± 2.453$^{\Delta\Delta}$	1.031 ± 0.385
Heart	Dss	ig	0.25	0.036 ± 0.014	8.070 ± 2.207	5.508 ± 1.583
		io-solution	0.083	0.115 ± 0.097	8.601 ± 0.712	1.138 ± 0.147
		io-gel	1	0.141 ± 0.051	12.210 ± 1.745	0.397 ± 0.128
	Rg_1	ig	0.5	0.011 ± 0.005	0.823 ± 0.228	0.932 ± 0.607
		io-solution	0.083	0.074 ± 0.039	4.916 ± 1.454**	1.683 ± 0.141
		io-gel	9	0.016 ± 0.007	7.236 ± 2.936	33.625 ± 1.668
Liver	Dss	ig	1	0.028 ± 0.014	5.726 ± 0.221	4.386 ± 0.279
		io-solution	0.083	0.376 ± 0.163**	9.151 ± 1.081	8.834 ± 1.874
		io-gel	1	0.183 ± 0.095	23.843 ± 4.228$^{\Delta}$	1.531 ± 0.105$^{\Delta}$
	Rg_1	ig	1	0.016 ± 0.002	2.568 ± 0.630	2.554 ± 0.166
		io-solution	0.083	0.200 ± 0.129**	5.350 ± 1.448	4.201 ± 1.355
		io-gel	1	0.029 ± 0.017$^{\Delta\Delta}$	5.519 ± 0.066	1.715 ± 0.546$^{\Delta}$
Spleen	Dss	ig	0.5	0.038 ± 0.005	9.058 ± 1.848	12.330 ± 1.813
		io-solution	0.5	0.049 ± 0.023	1.875 ± 0.418**	1.080 ± 0.171
		io-gel	3	0.021 ± 0.011	-	-
	Rg_1	ig	0.083	0.036 ± 0.009	6.231 ± 1.819	6.530 ± 1.455
		io-solution	0.5	0.115 ± 0.016**	8.032 ± 1.731	1.490 ± 0.520
		io-gel	0.083	0.039 ± 0.013$^{\Delta\Delta}$	-	-
Lung	Dss	ig	0.25	0.022 ± 0.009	2.194 ± 0.695	3.342 ± 1.278
		io-solution	0.25	0.131 ± 0.045**	6.960 ± 0.340**	1.363 ± 0.862
		io-gel	0.5	0.041 ± 0.013$^{\Delta\Delta}$	6.072 ± 1.883	0.741 ± 0.106
	Rg_1	ig	0.25	0.021 ± 0.008	2.998 ± 0.915	5.299 ± 1.205
		io-solution	0.25	0.271 ± 0.102**	18.477 ± 3.571**	2.115 ± 0.555
		io-gel	0.5	0.051 ± 0.018$^{\Delta\Delta}$	13.043 ± 2.702	1.328 ± 0.273
Kidney	Dss	ig	0.5	0.181 ± 0.027	55.650 ± 10.529	9.713 ± 2.164
		io-solution	0.083	0.264 ± 0.131	21.062 ± 3.879*	3.303 ± 0.053
		io-gel	1.5	0.037 ± 0.024$^{\Delta\Delta}$	12.419 ± 2.664	75.022 ± 36.979$^{\Delta}$
	Rg_1	ig	0.5	0.026 ± 0.012	3.595 ± 0.491	1.863 ± 0.698
		io-solution	0.083	0.122 ± 0.048**	10.845 ± 1.227**	19.525 ± 7.014
		io-gel	0.25	0.026 ± 0.013$^{\Delta\Delta}$	4.984 ± 1.631$^{\Delta\Delta}$	5.499 ± 2.455

$^{*}P < 0.05$, $^{**}P < 0.01$, *versus* the intragastric solution group;

$^{\Delta}P < 0.05$, $^{\Delta\Delta}P < 0.01$, *versus* the ophthalmic solution group

ig: intragastric solution; io-solution: ophthalmic solution; io-gel: ophthalmic ISG

$t_{1/2}$ (10.814 ± 1.853 h) of Dss in the brain tissue in the ophthalmic drop group were significantly different from those in the intragastric group ($AUC_{0\text{-}t}$: 1.796 ± 0.196 mg/L·min; $t_{1/2}$: 3.454 ± 2.041 h). The $AUC_{0\text{-}t}$ of Rg_1 in the intragastric group and ophthalmic drop group were 0.414 ± 0.0643 mg/L·min and 3.148 ± 0.537 mg/L·min, respectively ($^{*}P < 0.05$). The $AUC_{0\text{-}t}$ of Dss and Rg_1 in the CSOT-ISG group were 12.783 ± 3.642 mg/L·min and 9.491 ± 2.453 mg/L·min,

respectively, which indicated highly significant differences when compared with those of the ophthalmic drop group.

The concentration–time curves of Dss and Rg_1 in the heart of SD rats are displayed in Fig. 7, and the relevant pharmacokinetic parameters are summarized in Table VI. Compared to the intragastric group, the C_{max} of Dss in the heart in the ophthalmic drop group was increased, while the $AUC_{0\text{-}t}$ was comparable to that in the intragastric group. The $AUC_{0\text{-}t}$ values of Rg_1 in the intragastric and ophthalmic drop groups were 0.823 ± 0.228 mg/L·min

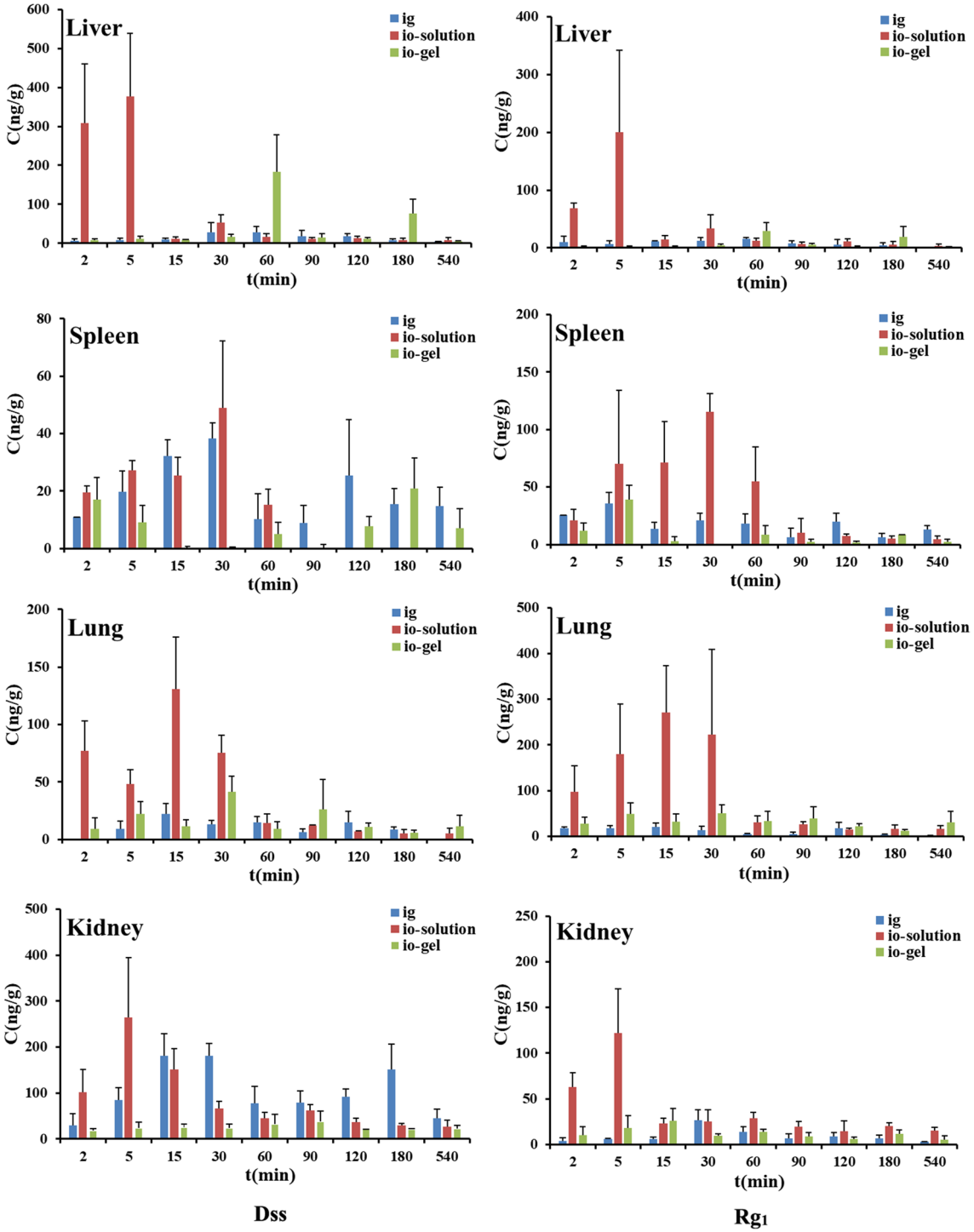

Fig. 8 Concentrations of Dss and Rg_1 in different tissues (mean ± *SD*, n = 5; ig: intragastric solution; io-solution: ophthalmic solution; io-gel: ophthalmic ISG)

and 4.916 ± 1.454 mg/L·min, respectively ($^{*}P < 0.01$). The treatment of CSOT-ISG raised the $AUC_{0\text{-}t}$ of Dss and Rg_1 compared to those in the ophthalmic drop group.

The content analysis of Dss and Rg_1 in the liver, spleen, lung, and kidney tissues of rats are displayed in Fig. 8, and the relevant pharmacokinetic parameters are given in Table VI. Compared with the intragastric group, the C_{max} of Dss in the liver and lungs in the ophthalmic drop group were larger and the $AUC_{0\text{-}t}$ of Dss in the lung also increased. The $AUC_{0\text{-}t}$ of Dss in the spleen and kidneys in the ophthalmic drop group were lower than those in the intragastric group. The content of Dss in the spleen in the ophthalmic drop group was below the quantitative lower limit after 60 min of administration. Following ophthalmic drop administration, the C_{max} of Rg_1 in the liver, spleen, lung, and kidney tissues were greater than those in the intragastric group, and the $AUC_{0\text{-}t}$ of Rg_1 in the lung and kidney tissues from the ophthalmic drop group were higher than those in the intragastric group ($^{*}P < 0.05$). Compared with the ophthalmic drop group, the CSOT-ISG group exhibited a significantly greater $AUC_{0\text{-}t}$ of Dss in liver. However, the C_{max} and $AUC_{0\text{-}t}$ of Dss in tissues from the spleen, lung, and kidney were decreased in the CSOT-ISG group. The C_{max} of Rg_1 in every tissue in the CSOT-ISG group was noticeably lower than that of tissues in the ophthalmic drop group. The $AUC_{0\text{-}t}$ of Rg_1 in every tissue in the CSOT-ISG group also decreased, with the kidney exhibiting the greatest reduction. The tissue concentrations of Dss and Rg_1 in the spleen in the CSOT-ISG group were extremely low, and could not be detected at some time points; hence, the $AUC_{0\text{-}t}$ and $t_{1/2}$ could not be calculated.

Tissue Distribution and Targeted Parameters

This study compared the targeting of two index components in various tissues using different routes of administration (Table VII).

According to the size of the *Te*, the distribution results of Dss in the intragastric group were in the following order: kidney, spleen, heart, liver, lung, and brain; and the distribution pattern of Rg_1 was as follows: spleen > kidney > lung > liver > heart > brain. The predominant site of Dss distribution was the kidney, which is similar to the report by other researchers [41, 42]. Rg_1 levels in the brain were low, which is consistent with the findings of other researchers [43]. The distribution results of Dss in the ophthalmic drop group were in the following order: kidney, liver, heart, lung, brain, and spleen; and the distribution pattern of Rg_1 was as follows: lung > kidney > spleen > liver > heart > brain. The distribution results of Dss in the CSOT-ISG group were in the following order: (first through fifth) liver, brain, kidney, heart, and lung; and the distribution pattern of Rg_1 was as follows: lung, brain, heart, liver, and kidney.

According to the size of the *TI* and *Rte*, the drug-targeting effects of Dss and Rg_1 in the brain, heart, and lung tissues obtained from the ophthalmic drop group were superior to those obtained from similar samples in the intragastric group. The targeting effects of Dss and Rg_1 in the brain, heart, and liver tissues in the CSOT-ISG group were better than those in the ophthalmic drop group, indicating that CSOT-ISG was highly targeted in the heart and brain and could reduce the toxic side effects of drugs in the lungs and kidneys. As a result, the targeting effects of Dss and Rg_1 in the heart and brain were found to be higher than those in other tissues, which further supported the conclusion that

Table VII Targeting Parameters of Dss and Rg_1 in Rat Tissues after Administration of Different Preparations

Compound	Tissue	*Te*/%			*TI*		*Rte*	
		ig	io-solution	io-gel	ig *vs* io-solution	io-solution *vs* io-gel	ig *vs* io-solution	io-solution *vs* io-gel
Dss	Brain	2.18	9.60	18.99	2.82	2.53	3.41	0.98
	Heart	9.78	16.32	18.14	1.07	1.42	0.67	0.11
	Liver	6.94	17.36	35.41	1.60	2.61	1.50	1.04
	Spleen	10.98	3.56	/	0.21	/	−0.68	/
	Lung	2.66	13.20	9.02	3.17	0.87	3.96	−0.32
	Kidney	67.46	39.96	18.45	0.38	0.59	−0.41	−0.54
Rg_1	Brain	2.49	6.20	23.57	7.60	3.01	1.49	2.80
	Heart	4.95	9.68	17.97	5.97	1.47	0.96	0.86
	Liver	15.44	10.54	13.71	2.08	1.03	−0.32	0.30
	Spleen	37.47	15.82	/	1.29	/	−0.58	/
	Lung	18.03	36.39	32.39	6.16	0.71	1.02	−0.11
	Kidney	21.62	21.36	12.38	3.02	0.46	−0.01	−0.42

ig: intragastric solution; io-solution: ophthalmic solution; io-gel: ophthalmic ISG

the compound *Salvia* recipe could be used mainly for the management of cardiovascular and cerebrovascular diseases.

Discussion

The clinical preparations of compound *Salvia* recipe are utilised mainly to treat angina pectoris and coronary heart diseases [44, 45]. Although several studies have demonstrated the efficacy of the compound *Salvia* recipe in the treatment of cerebrovascular diseases [46, 47], there is no relevant preparation study. Therefore, in this study, we aimed to prepare a compound *Salvia* ophthalmic thermosensitive ISG for the treatment these diseases.

In a previous experiment, we compared the levels of three commonly used indicator components of *Panax notoginseng* total saponins (Panax notoginseng saponin R_1, ginsenoside Rb_1, and ginsenoside Rg_1) [48, 49] in traditional Chinese medicine extract solution and the drug concentration in rats. The experiment revealed a high concentration of ginsenoside Rg_1 in both the extract solution and tissue samples of rats, leading to the selection of ginsenoside Rg_1 as the indicator component of Panax notoginseng, and this is consistent with the findings of prior studies [50, 51]. Additionally, the *in vitro* and *in vivo* chromatographic conditions established in this paper can also be used for the determination of Panax notoginseng saponin R_1 and ginsenoside Rb_1.

P407 has obtained popularity as a polymer in ocular drug delivery systems due to its beneficial biocompatibility, low toxicity, and temperature sensitivity that is concentration-dependent [52, 53]. However, the temperature-sensitive gel prepared separately has a lower gelling temperature and its concentration fluctuates with body fluids. P407 concentration decreases due to dilution with body fluids. Furthermore, it can irritate mucous membranes and may lead to ocular hypertriglyceridemia when used in high concentrations [54]. Therefore, during the preparation of CSOT-ISG, it was combined with P188 and HPMC, which can effectively raise its gelling temperature [55] and ensure the formula exhibits sufficient gel strength [56] and exhibits the properties of sustained drug release.

At the beginning of the gel preparation, the effect of the addition form and order of the compound *Salvia* recipe were investigated. The freeze-dried powder of compound *Salvia* is highly hygroscopic and easily adhesive at room temperature, and this could affect precise weighing during preparation. Therefore, a water-extract solution was used in later studies. Additionally, we encountered some challenges when directly dissolving the polymer in the water-extract solution, such as a long polymer dissolution time and large differences in GT. Finally, the COST-ISG was prepared by mixing water-extract solution (50%, w/w) into a gel matrix [57], which ensured high drug content and high efficiency of the gel prepared.

The normal pH range of tears is 6.5–7.6, hence ocular preparations within this pH range are less likely to irritate the eyes [58]. The pH of the compound *Salvia miltiorrhiza* water-extract solution was adjusted to a neutral pH in earlier studies. In order to find out how the addition of excipients and compound *Salvia miltiorrhiza* water-extract solution affected the pH value of the gel during its preparation, the pH values of the blank gel and COST-ISG were measured in this experiment. The pH values of the blank gel and COST-ISG were 7.03 ± 0.02 and 6.97 ± 0.05, respectively, indicating that the addition of excipients and extract solution had no impact on the pH values of the gel, and that the prepared COST-ISG satisfied the pH requirements of ophthalmic preparation.

Furthermore, the residence time of the ocular formulation on the precorneal surface was impacted by its viscosity, which is an important element that needs to be considered when increasing the residence time [59]. The viscosity of the gel before dilution with artificial tears (room temperature) was 1440.0 ± 27.00 mPa·s, and the viscosity after dilution with artificial tears (physiological conditions) was 5956.7 ± 130.35 mPa·s. The lower viscosity of the gel at room temperature facilitates the administration of the drug. The gel's viscosity was increased under ocular physiological conditions, which is conducive to the retention of the drug after ocular administration.

The current research methods for the *in vitro* release of gels include the membrane-less method [60], the dialysis bag method [61], and the diffusion cell method [62, 63]. The dialysis bag method involves gradual drug exchange with the release medium through the dialysis bag, potentially leading to the drug not being in a complete leakage groove. In the diffusion cell method, the area of the semipermeable membrane is relatively fixed, which limits its ability to mimic the effect of blinking on drug permeation after drug administration. The membrane-free dissolution method does not require the use of a semi-permeable membrane. This technique has also been extensively employed to investigate the *in vitro* release of ocular thermosensitive gels. This technique is more appropriate for simulating the real situation of the gel in the eye, as it can simulate the blink shearing impact of tears on the gel after it is *in situ* under the oscillation of a constant-temperature oscillator. Therefore, the *in vitro* release of Dss and Rg_1 from the CSOT-ISG was studied by the membrane-free technique.

During the pretreatment of samples, we investigated the effect of the protein precipitation method [51] on the extraction efficiency of Dss and Rg_1. The extraction rate of Dss and Rg_1 was low when using various protein precipitates, and the lower limit of quantification was insufficient for *in vivo* research in rats. Therefore, we explored the liquid–liquid extraction method [41, 64] for improved extraction efficiency.

This study investigated the impact of acidifying reagents, specifically acetic ether and perchloric acid, as extraction solvents on the extraction effectiveness of Dss and Rg_1. Our findings reveal that the extraction recovery of Rg_1 is notably low. Further investigation also revealed that the use of *N*-butanol-ethyl acetate (1:4, v/v) [65] could significantly enhance the extraction recovery of both Dss and Rg_1, resulting in an 80% extraction recovery rate. Moreover, a lower limit of quantification is also sufficient for subsequent experiments.

Pharmacokinetics plays an essential role in the assessment of drug effects [66]. Based on pharmacokinetic findings, it can be seen that the $AUC_{0\text{-}t}$ of Dss in plasma after intragastric or eye drops of the compound *Salvia* extract solution in rats were not significantly different, and the $t_{1/2}$ of the eye drops group was significantly shorter than that of the intragastric group, which may be related to the rapid absorption of the drug through the ocular mucosa and the greater loss of the eye drops due to factors, such as nasolacrimal duct drainage, blinking, and lacrimation [17, 29]. With the exceptions of the kidney (excretory organ) and spleen (blood storage organ), the highest content of Dss was found in the heart after intragastric administration, which is consistent with the fact that the oral preparations of compound *Salvia miltiorrhiza* are primarily utilized in the management of coronary heart disease and angina pectoris in the clinic [67]. Moreover, a notable improvement in drug absorption was observed when compound *Salvia* extract solution was prepared in COST-ISG for ocular application. The prepared COST-ISG has strong targeting abilities on the heart and brain, which is important for the clinical application of the compound *Salvia* recipe.

Conclusion

In the present study, P407, P188, and HPMC (17.85%: 6.31%: 0.21% w/w) were used to develop a compound *Salvia* ophthalmic thermosensitive ISG (CSOT-ISG) for ocular administration. The gel was kept in a flowing liquid condition with low viscosity at room temperature and rapidly changed into a semi-solid scenario when exposed to ocular physiological temperature, which is advantageous for ocular applications. The CSOT-ISG's pH, viscosity, and GT all complied with the specifications of ophthalmic preparations. The outcomes of *in vitro* release and erosion investigations showed that Dss and Rg_1 in the gel were primarily released by erosion. Histopathological examination of the rabbit eyes also found that CSOT-ISG was safe and reliable, and could be used for ocular drugs delivery. *In vivo* studies in rats demonstrated that CSOT-ISG had strong targeting to the heart and brain tissues, and could reduce the accumulation of drugs in the spleen, lungs, and kidneys, thereby reducing side effects. Overall, CSOT-ISG shows potential as a drug delivery method for the management of cardiovascular and cerebrovascular illnesses through ocular administration.

Supplementary Information The online version contains supplementary material available at https://doi.org/10.1208/s12249-024-02913-8.

Acknowledgements The authors gratefully acknowledge the support from the Natural Science Foundation of Anhui Province (grant Number 2108085MH312). Thanks for the language assistance provided by Charlesworth Group.

Author Contributions **Yanqiu Long:** Conceptualization, Methodology, Investigation, Writing—original draft, Writing—review & editing. **Fang Lei:** Investigation,Visualization, Writing—original draft, Writing—review & editing. **Jie Hu:** Project administration, Writing—review & editing. **Zhiyun Zheng:** Conceptualization, Writing—review & editing, Supervision. **Shuangying Gui:** Conceptualization, Writing—review & editing. **Ning He:** Conceptualization, Writing—review & editing, Supervision, Funding acquisition. All authors read and approved the final manuscript.

Funding This work was supported by the Anhui Provincial Natural Science Foundation [grant number 2108085MH312].

Data availability Data will be made available on request.

Declarations

Competing Interest The authors declare that they have no known competing financial interests or personal relationships that could have appeared to influence the work reported in this paper.

References

1. Chu Y, Zhang L, Wang X, Guo J, Guo Z, Ma X. The effect of Compound Danshen Dripping Pills, a Chinese herb medicine, on the pharmacokinetics and pharmacodynamics of warfarin in rats. J Ethnopharmacol. 2011;137(3):1457–61. https://doi.org/10.1016/j.jep.2011.08.035.
2. Luo J, Song W, Yang G, Xu H, Chen K. Compound Danshen (Salvia miltiorrhiza) Dripping Pill for Coronary Heart Disease: An Overview of Systematic Reviews. Am J Chin Med. 2015;43(01):25–43. https://doi.org/10.1142/s0192415x15500020.
3. Li Y. Study on composition and pharmacological effect of compound Saliva miltiorrhiza prescription. Drug Evaluation. 2020;17(4):25–6. https://doi.org/10.3969/j.issn.1672-2809.2020.04.008.
4. Wang L, Ma R, Liu C, Liu H, Zhu R, Guo S, et al. Salvia miltiorrhiza: A Potential Red Light to the Development of Cardiovascular Diseases. Curr Pharm Des. 2017;23(7):1077–97. https://doi.org/10.2174/1381612822666161010105242.
5. Hao C, Li Z, Zhang M, Han B. Research progress of Salvia miltiorrhiza and its compatible preparations in treatment of coronary heart disease. Chin Tradit Herbal Drugs. 2021;52(13):4096–106. https://doi.org/10.7501/j.issn.0253-2670.2021.13.033.
6. Su X, Yao Z, Li S, Sun H. Synergism of Chinese Herbal Medicine: Illustrated by Danshen Compound. Evid Based Complement Alternat Med. 2016;2016:1–10. https://doi.org/10.1155/2016/7279361.
7. Chen Z-x, Xu Q-q, Shan C-s, Shi Y-h, Wang Y, Chang RC-C, et al. Borneol for Regulating the Permeability of the Blood-Brain

Barrier in Experimental Ischemic Stroke: Preclinical Evidence and Possible Mechanism. Oxidative Med Cell Longev. 2019;2019:1–15. https://doi.org/10.1155/2019/2936737.
8. Zhang J, Liu S-L, Wang H, Shi L-Y, Li J-P, Jia L-J, et al. The effects of borneol on the pharmacokinetics and brain distribution of tanshinone IIA, salvianolic acid B and ginsenoside Rg1 in Fufang Danshen preparation in rats. Chin J Nat Med. 2021;19(2):153–60. https://doi.org/10.1016/s1875-5364(21)60016-x.
9. Yuan Y, Zhang H, Ma W, Sun S, Wang B, Zhao L, et al. Influence of compound danshen tablet on the pharmacokinetics of losartan and its metabolite EXP3174 by liquid chromatography coupled with mass spectrometry. Biomed Chromatogr. 2013;27(9):1219–24. https://doi.org/10.1002/bmc.2930.
10. Zhao Y, Jing L. Study on further optimization of prescription of compound danshen composite. Zhong guo Zhong Yao Za Zhi. 2011;17:2437–40. https://doi.org/10.4268/cjcmm20111728.
11. Zhang B, Gao X, Shang H, Zhao Y, Wang Y. Study on pharmaceutical matters and functional mechanisms of complex prescriptions of Radix Salvial Milti orrhizal. World J Sci Technol. 2003;5(5):14–7. https://doi.org/10.3969/j.issn.1674-3849.2003.05.004.
12. Li Z-m, Xu S-w, Liu P-q. Salvia miltiorrhizaBurge (Danshen): a golden herbal medicine in cardiovascular therapeutics. Acta Pharmacol Sin. 2018;39(5):802–24. https://doi.org/10.1038/aps.2017.193.
13. Zeng G, Xu Q, Xiao H, Liang X. Influence of compatibility ratio of Fufang Danshen on the dissolution of Danshen compositions. Se Pu. 2004;22(2):141–3. https://doi.org/10.3321/j.issn:1000-8713.2004.02.012.
14. Lei F, Wu D, Fei Q, Luo R, He N. Optimization of water extraction for Salviae Miltiorrhizae Radix et Rhizoma and Notoginseng Radix et Rhizoma in compound Salvia recipe by orthogonal design and AHP-CRITIC method. Cent South Pharm. 2022;20(3):551–6. https://doi.org/10.7539/j.issn.1672-2981.2022.03.012.
15. Willoughby CE, Ponzin D, Ferrari S, Lobo A, Landau K, Omidi Y. Anatomy and physiology of the human eye: Effects of mucopolysaccharidoses disease on structure and function - a review. Clin Exp Ophthalmol. 2010;38(Suppl. 1):2–11. https://doi.org/10.1111/j.1442-9071.2010.02363.x.
16. Urtti A. Challenges and obstacles of ocular pharmacokinetics and drug delivery. Adv Drug Deliv Rev. 2006;58(11):1131–5. https://doi.org/10.1016/j.addr.2006.07.027.
17. Gaudana R, Ananthula HK, Parenky A, Mitra AK. Ocular Drug Delivery. AAPS J. 2010;12(3):348–60. https://doi.org/10.1208/s12248-010-9183-3.
18. Chiou G. Systemic delivery of polypeptide drugs through ocular route. J Ocul Pharmacol. 1994;10(1):93–9. https://doi.org/10.1089/jop.1994.10.93.
19. Huang T, Fan Y, Liu R. Ocular routes of insulin administration. China Med Herald. 2007;4(27):161. https://doi.org/10.3969/j.issn.1673-7210.2007.27.12.
20. Volotinen M, Hakkola J, Pelkonen O, Vapaatalo H, Mäenpää J. Metabolism of Ophthalmic Timolol: New Aspects of an Old Drug. Basic Clin Pharmacol Toxicol. 2011;108(5):297–303. https://doi.org/10.1111/j.1742-7843.2011.00694.x.
21. Mäenpää J, Pelkonen O. Cardiac safety of ophthalmic timolol. Expert Opin Drug Saf. 2016;15(11):1549–61. https://doi.org/10.1080/14740338.2016.1225718.
22. Shiuey Y, Eisenberg M. Cardiovascular effects of commonly used ophthalmic medications. Clin Cardiol. 1996;19(1):5–8. https://doi.org/10.1002/clc.4960190104.
23. Li M. Four cases of heart attack induced by eye-dotting with Shuangxingming eye drops. Chinese J Optom Ophthalmol Vis Sci. 2003;5(2):113. https://doi.org/10.3760/cma.j.issn.1674-845X.2003.02.026.
24 Dai M, Bai L, Zhang H, Ma Q, Luo R, Lei F, et al. A novel flunarizine hydrochloride-loaded organogel for intraocular drug delivery in situ: Design, physicochemical characteristics and inspection. Int J Pharm. 2020;576:119027. https://doi.org/10.1016/j.ijpharm.2020.119027.
25. Bai L, Fei Q, Lei F, Luo R, Ma Q, Dai M, et al. Comparative analysis of pharmacokinetics of vancomycin hydrochloride in rabbits after ocular, intragastric, and intravenous administration by LC-MS/MS. Xenobiotica. 2020;50(12):1461–8. https://doi.org/10.1080/00498254.2020.1774681.
26. Li F, Fei Q, Mao D, Si Q, Dai M, Ma Q, et al. Comparative Pharmacokinetics of Nimodipine in Rat Plasma and Tissues Following Intraocular, Intragastric, and Intravenous Administration. AAPS PharmSciTech. 2020;21(6):1. https://doi.org/10.1208/s12249-020-01772-3.
27. Ma Q, Luo R, Zhang H, Dai M, Bai L, Fei Q, et al. Design, Characterization, and Application of a pH-Triggered In Situ Gel for Ocular Delivery of Vinpocetine. AAPS PharmSciTech. 2020;21(7):1–1. https://doi.org/10.1208/s12249-020-01791-0.
28. Mao D, Li F, Ma Q, Dai M, Zhang H, Bai L, et al. Intraocular administration of tetramethylpyrazine hydrochloride to rats: a direct delivery pathway for brain targeting? Drug Deliv. 2019;26(1):841–8. https://doi.org/10.1080/10717544.2019.1650849.
29. Jumelle C, Gholizadeh S, Annabi N, Dana R. Advances and limitations of drug delivery systems formulated as eye drops. J Control Release. 2020;321:1–22. https://doi.org/10.1016/j.jconrel.2020.01.057.
30. Wu Y, Liu Y, Li X, Kebebe D, Zhang B, Ren J, et al. Research progress of in-situ gelling ophthalmic drug delivery system. Asian J Pharm Sci. 2019;14(1):1–15. https://doi.org/10.1016/j.ajps.2018.04.008.
31. Mura P, Mennini N, Nativi C, Richichi B. In situ mucoadhesive-thermosensitive liposomal gel as a novel vehicle for nasal extended delivery of opiorphin. Eur J Pharm Biopharm. 2018;122:54–61. https://doi.org/10.1016/j.ejpb.2017.10.008.
32. Wang L, Pan H, Gu D, Li P, Su Y, Pan W. A composite System Combining Self-Targeted Carbon Dots and Thermosensitive Hydrogels for Challenging Ocular Drug Delivery. J Pharm Sci. 2022;111(5):1391–400. https://doi.org/10.1016/j.xphs.2021.09.026.
33. Qi H, Chen W, Huang C, Li L, Chen C, Li W, et al. Development of a poloxamer analogs/carbopol-based in situ gelling and mucoadhesive ophthalmic delivery system for puerarin. Int J Pharm. 2007;337(1–2):178–87. https://doi.org/10.1016/j.ijpharm.2006.12.038.
34. Huang W, Zhang N, Hua H, Liu T, Tang Y, Fu L, et al. Preparation, pharmacokinetics and pharmacodynamics of ophthalmic thermosensitive in situ hydrogel of betaxolol hydrochloride. Biomed Pharmacother. 2016;83:107–13. https://doi.org/10.1016/j.biopha.2016.06.024.
35. Bai L, Lei F, Luo R, Fei Q, Zheng Z, He N, et al. Development of a Thermosensitive In-Situ Gel Formulations of Vancomycin Hydrochloride: Design, Preparation, In Vitro and In Vivo Evaluation. J Pharm Sci. 2022;111(9):2552–61. https://doi.org/10.1016/j.xphs.2022.04.011.
36. Gugleva V, Titeva S, Ermenlieva N, Tsibranska S, Tcholakova S, Rangelov S, et al. Development and evaluation of doxycycline niosomal thermoresponsive in situ gel for ophthalmic delivery. Int J Pharm. 2020;591:120010. https://doi.org/10.1016/j.ijpharm.2020.120010.
37. Zeng Y, Chen J, Li Y, Huang J, Huang Z, Huang Y, et al. Thermosensitive gel in glaucoma therapy for enhanced bioavailability: In vitro characterization, in vivo pharmacokinetics and pharmacodynamics study. Life Sci. 2018;212:80–6. https://doi.org/10.1016/j.lfs.2018.09.050.

38. Yang Z, Nie S, Hsiao WLW, Pam W. Thermoreversible Pluronic® F127-based hydrogel containing liposomes for the controlled delivery of paclitaxel: in vitro drug release, cell cytotoxicity, and uptake studies. Int J Nanomed. 2011. https://doi.org/10.2147/ijn.S15057.
39. Luo Y, Yang W, Haji AA. Tissue distribution and targeting of Magnetic Nano-liposomes of SesquiterpeneRich Fraction from Cichorium glandulosum in mice. Drugs & Clinic. 2019;34(01):5–10. https://doi.org/10.7501/j.issn.1674-5515.2019.01.002.
40. Zhou J, OuYang Y, Xu Q, Wu H. Prepare of Baicalin Solid Lipid Nanoparticles and Its Tissue Distribution in Mice. J Anhui Tradit Chin Med Coll. 2020;39(03):72–7. https://doi.org/10.3969/j.issn.2095-7246.2020.03.018.
41. Meng X, Jiang J, Pan H, Wu S, Wang S, Lou Y, et al. Preclinical Absorption, Distribution, Metabolism, and Excretion of Sodium Danshensu, One of the Main Water-Soluble Ingredients in Salvia miltiorrhiza, in Rats. Front Pharmacol. 2019;10:554. https://doi.org/10.3389/fphar.2019.00554.
42. Liu J, Zhao X, Zhang L, Fang M, Sun W, Zheng X. Co-administration of Radix curcumae alters the tissue distribution of danshensu in Radix salviae miltiorrhiae in rabbits. Am J Chin Med. 2008;36(5):929–38. https://doi.org/10.1142/S0192415X08006351.
43. Wang S, Zang W, Zhao X, Feng W, Zhao M, He X, et al. Effects of Borneol on Pharmacokinetics and Tissue Distribution of Notoginsenoside R1 and Ginsenosides Rg1 and Re in Panax notoginsengin Rabbits. J Anal Methods Chem. 2013;2013:1–11. https://doi.org/10.1155/2013/706723.
44. Jia Y, Huang F, Zhang S, Leung S. Is danshen (Salvia miltiorrhiza) dripping pill more effective than isosorbide dinitrate in treating angina pectoris? A systematic review of randomized controlled trials. Int J Cardiol. 2012;157(3):330–40. https://doi.org/10.1016/j.ijcard.2010.12.073.
45. Jia Y, Leung S. How Efficacious is Danshen (Salvia miltiorrhiza) Dripping Pill in Treating Angina Pectoris? Evidence Assessment for Meta-Analysis of Randomized Controlled Trials. J Altern Complement Med. 2017;23(9):676–84. https://doi.org/10.1089/acm.2017.0069.
46. Zhang X, Qian S, Zhang Y, Wang R. Salvia miltiorrhiza: A source for anti-Alzheimer's disease drugs. Pharm Biol. 2016;54(1):18–24. https://doi.org/10.3109/13880209.2015.1027408.
47. Zhou L, Zuo Z, Chow MSS. Danshen: an overview of its chemistry, pharmacology, pharmacokinetics, and clinical use. J Clin Pharmacol. 2005;45(12):1345–59. https://doi.org/10.1177/0091270005282630.
48. Zheng D, Chu Y, Li S, Zhou S, Li W, Xie Y, et al. Enhancing effect of borneol on pharmacokinetics of ginsenoside Rb1, ginsenoside Rg1, and notoginsenoside R1 in healthy volunteers after oral administration of compound Danshen dropping pills. Biomed Chromatogr. 2022;36(5):e5311. https://doi.org/10.1002/bmc.5311.
49. Zheng Y, Bai J, Li X, An Y, Li L, Wen T, et al. Biosynthesis and pharmacokinetics of Panax notoginseng enteric-coated soft capsules. Ann Transl Med. 2023;11(2):51. https://doi.org/10.21037/atm-22-5751.
50. Wang D, Koh H, Hong Y, Zhu H, Xu M, Zhang Y, et al. Chemical and morphological variations of Panax notoginseng and their relationship. Phytochemistry. 2013;93:88–95. https://doi.org/10.1016/j.phytochem.2013.03.007.
51. Fu X, Chen K, Li Z, Fan H, Xu B, Liu M, et al. Pharmacokinetics and Oral Bioavailability of Panax Notoginseng Saponins Administered to Rats Using a Validated UPLC–MS/MS Method. J Agric Food Chem. 2022;71(1):469–79. https://doi.org/10.1021/acs.jafc.2c06312.
52. Soliman KA, Ullah K, Shah A, Jones DS, Singh TRR. Poloxamer-based in situ gelling thermoresponsive systems for ocular drug delivery applications. Drug Discov Today. 2019;24(8):1575–86. https://doi.org/10.1016/j.drudis.2019.05.036.
53. Patel N, Thakkar V, Metalia V, Baldaniya L, Gandhi T, Gohel M. Formulation and development of ophthalmic in situ gel for the treatment ocular inflammation and infection using application of quality by design concept. Drug Dev Ind Pharm. 2016;42(9):1406–23. https://doi.org/10.3109/03639045.2015.1137306.
54. Khallaf AM, El-Moslemany RM, Ahmed MF, Morsi MH, Khalafallah NM. Exploring a Novel Fasudil-Phospholipid Complex Formulated as Liposomal Thermosensitive in situ Gel for Glaucoma. Int J Nanomedicine. 2022;17:163–81. https://doi.org/10.2147/IJN.S342975.
55. Chu K, Chen L, Xu W, Li H, Zhang Y, Xie W, et al. Preparation of a Paeonol-Containing Temperature-Sensitive In Situ Gel and Its Preliminary Efficacy on Allergic Rhinitis. Int J Mol Sci. 2013;14(3):6499–515. https://doi.org/10.3390/ijms14036499.
56. Morsi N, Ghorab D, Refai H, Teba H. Ketoroloac tromethamine loaded nanodispersion incorporated into thermosensitive in situ gel for prolonged ocular delivery. Int J Pharm. 2016;506(1–2):57–67. https://doi.org/10.1016/j.ijpharm.2016.04.021.
57. He M, Zhao C, Li J, Zhao Y, Wu H, Chen M. Preparation of compound Chinese medicine gels. Chin J Vet Med. 2019;55(3):50–3.
58. Modi D, Warsi MH, Mohammad, Garg V, Bhatia M, Kesharwani P, et al. Formulation development, optimization, and in vitro assessment of thermoresponsive ophthalmic pluronic F127-chitosan in situ tacrolimus gel. J Biomater Sci Polym Ed. 2021;32(13):1678–702. https://doi.org/10.1080/09205063.2021.1932359.
59. Sun J, Sun X. Preparation of a novel tacrolimus ion sensitive ocular in situ gel and in vivo evaluation of curative effect of immune conjunctivitis. Pharm Dev Technol. 2022;27(4):399–405. https://doi.org/10.1080/10837450.2022.2067870.
60. Yu Z-G, Geng Z-X, Liu T-F, Jiang F. In vitro and in vivo evaluation of an in situ forming gel system for sustained delivery of Florfenicol. J Vet Pharmacol Ther. 2015;38(3):271–7. https://doi.org/10.1111/jvp.12171.
61. Cao Z, Chen Y, Bai S, Zheng Z, Liu Y, Gui S, et al. In situ formation of injectable organogels for punctal occlusion and sustained release of therapeutics: design, preparation, in vitro and in vivo evaluation. Int J Pharm. 2023;638:122933. https://doi.org/10.1016/j.ijpharm.2023.122933.
62. Makwana SB, Patel VA, Parmar SJ. Development and characterization of in-situ gel for ophthalmic formulation containing ciprofloxacin hydrochloride. Results Pharma Sci. 2015;6:1–6. https://doi.org/10.1016/j.rinphs.2015.06.001.
63. Nair AB, Shah J, Jacob S, Al-Dhubiab BE, Sreeharsha N, Morsy MA, et al. Experimental design, formulation and in vivo evaluation of a novel topical in situ gel system to treat ocular infections. PLoS ONE. 2021;16(3):e0248857. https://doi.org/10.1371/journal.pone.0248857.
64. Pan G, Zhang B, Gao X. Determination of danshensu in rat serum after oral administer compound Salvia recipe. Zhongguo Zhong Yao Za Zhi. 2003;28(6):562–5. https://doi.org/10.3321/j.issn:1001-5302.2003.06.027.
65. Jin T, Liu Z, Chu Y, Ma X, Li S, Wang X, et al. UFLC–MS/MS Determination and Population Pharmacokinetic Study of Tanshinol, Ginsenoside Rb1 and Rg1 in Rat Plasma After Oral Administration of Compound Danshen Dripping Pills. Eur J Drug Metab Pharmacokinet. 2020;45(4):523–33. https://doi.org/10.1007/s13318-020-00618-4.

66. Jin Y, Yu L, Xu F, Zhou J, Xiong B, Tang Y, et al. Pharmacokinetics of Active Ingredients of Salvia miltiorrhiza and Carthamus tinctorius in Compatibility in Normal and Cerebral Ischemia Rats: A Comparative Study. Eur J Drug Metab Pharmacokinet. 2020;45(2):273–84. https://doi.org/10.1007/s13318-019-00597-1.
67. Shan X, Hong B, Liu J, Wang G, Chen W, Yu N, et al. Review of chemical composition, pharmacological effects, and clinical application of Salviae Miltiorrhizae Radix et Rhizoma and prediction of its Q-markers. Zhongguo Zhong Yao Za Zhi. 2021;46(21):5496–511. https://doi.org/10.19540/j.cnki.cjcmm.20210630.203.